

Cite this: DOI: 00.0000/xxxxxxxxxx

Intuitive understanding of extinction of small particles in absorbing and active host media within the MLWA[†]

Anton D. Utyushev,^{*a} Vadim I. Zakomirnyi,^b Alexey A. Shcherbakov,^a Ilia L. Rasskazov^c and Alexander Moroz^dReceived Date
Accepted Date

DOI: 00.0000/xxxxxxxxxx

In an absorbing or an active host medium characterized by a complex refractive index $n_2 = n'_2 + in''_2$, our previously developed modified dipole long-wave approximation (MLWA) is shown to essentially overly with the exact Mie theory results for spherical nanoparticle with radius $a \lesssim 25$ nm ($a \lesssim 20$ nm) in the case of Ag and Au (Al and Mg) nanoparticles. The agreement for Au and Ag (Al and Mg) nanoparticles, slightly better in the case of Au than Ag, continues to be acceptable up to $a \sim 50$ nm ($a \sim 40$ nm), and can be used, at least qualitatively, up to $a \sim 70$ nm ($a \sim 50$ nm) correspondingly. A first order analytic perturbation theory (PT) in a normalized extinction coefficient, $\tilde{\kappa} = n''_2/n'_2$, around a nonabsorbing host is developed within the dipole MLWA and its properties are investigated. It is shown that, in a suitable parameter range, the PT can reliably capture the effect of host absorption or gain on the extinction efficiency of various plasmonic nanoparticles.

1 Introduction

Electromagnetic scattering in an absorbing host characterized by a complex refractive index $n_2 = n'_2 + in''_2$ (where n'_2 and n''_2 are real) has more than fifty years old history. The traditional scattering theory neglects the host dissipation and gain^{1,2}, because those cases imply either vanishing or infinite scattering wave at the spatial infinity. Once wave number $k = k' + ik''$ is a complex number, conventional expressions for cross sections cannot be straightforwardly extended for $k'' \neq 0$, because the expressions yield cross sections as *complex* quantities. Not surprisingly, the history of scattering in an absorbing host is filled in with a number of controversies^{3–19}. This is probably why in classical textbooks it is only fleetingly mentioned in Section 12.1.3 of ref. 2. Already the definition of an incident intensity is not straightforward, as the field incident on a particle is different at different points on the particle as a result of an absorbing medium^{4,5}. In an absorbing or an active unbounded host, the imaginary part k'' of the complex wave number $k = k' + ik'' = 2\pi n_2/\lambda_0$, where λ_0 is the *vacuum* wavelength, is nonzero, $k'' \neq 0$. A great deal of effort was required to arrive at suitable definitions of cross sections for $k'' \neq 0$.

In contrast to the conventional case of $k'' = 0$, two sets of cross

sections are commonly used: *inherent* and *apparent*. The former is obtained by performing surface integrals of corresponding Poynting vectors over the particle surface. The approach was developed a long time ago^{4,5}, but currently accepted expressions for the *inherent* cross-sections were not presented until 1999^{7–10}. The history of *apparent* cross sections, which are operationally defined in the far field, began with the optical theorem of Bohren and Gilra⁶. Here, too, it took a long time, until 2007, to arrive at definitive expressions for the apparent extinction cross-section cross section, C_{ext} , and the so-called apparent scattering cross section, C_{sca} ^{11–14}. A curious feature of the apparent extinction cross-section in an absorbing host is that it can be *negative*²⁰, which is neither an artifact of numerical simulations nor it violates any physical law. The apparent extinction cross-section quantifies the difference in the readings of a forward-scattering detector taken with and without the particle. If the surrounding medium is absorbing, the presence of the particle can in fact make the detector signal stronger, thereby implying a negative extinction cross-section. There is no violation of the energy conservation law, since in this case the extinction cross-section is not used to quantify the energy budget of a finite volume encompassing the particle²⁰. Another curiosity of apparent cross-sections in an absorbing host is that an intrinsic definition of an apparent absorption cross-sections, C_{abs} , is still missing. The difficulty lies in that the very presence of a particle necessarily modifies the near field around the particle. The latter may be the cause of an additional absorption in the host medium *outside* the particle compared to what is happening in the absence of the particle^{8,9}. The

^a School of Physics and Engineering, ITMO University, 197101, Saint-Petersburg, Russia

^b Beckman Institute for Advanced Science and Technology, University of Illinois at Urbana-Champaign, Urbana, IL 61801, USA

^c SunDensity Inc., Rochester, NY 14604, USA

^d Wave-scattering.com

* Corresponding author: ad.utyushev@gmail.com

† Electronic Supplementary Information (ESI) available: See DOI:

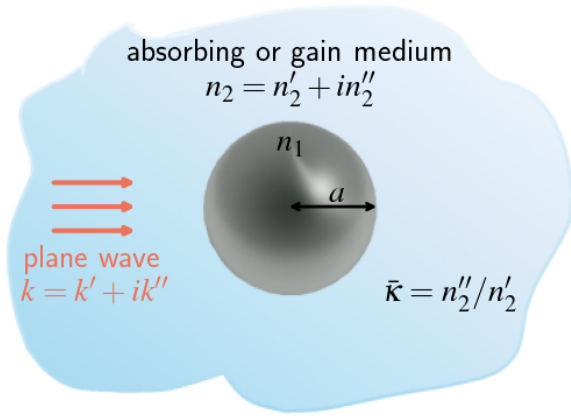


Fig. 1 Schematic representation of the problem under consideration. A spherical particle with radius a and refractive index n_1 is embedded in an absorbing or gain medium with $n_2 = n_2' + in_2''$, where n_2' and n_2'' are real. Imaginary refractive index of the host $n_2'' > 0$ for an absorbing medium and $n_2'' < 0$ for a gain medium, and $n_2'' = 0$ for a transparent medium. Normalized extinction coefficient $\bar{\kappa} = n_2''/n_2'$ is introduced to quantify the magnitude of the host dissipation or gain.

critical point is that because the field is disturbed by the particle, additional absorption may be realized in the medium external to the particle²¹.

First-principles far-field computations based on the general Lorenz–Mie theory showed that increasing absorption in the host medium *broadens* and suppresses plasmon resonances in the apparent extinction and effective scattering efficiency factors and suppresses resonance features in the phase function¹⁴. At the same time, using inherent cross-sections it was shown that a surrounding lossy medium can *narrow* the plasmonic resonances, as well as *increase* their amplitude dramatically^{15,17}. Given this recent revival of interest in the role of the host dissipation or gain on extinction cross sections with conflicting predictions of it either enhancing or reducing the localized surface plasmonic resonance (LSPR) of small particles^{14,15,17–19}, the focus of present work is on the apparent extinction cross-section C_{ext} in the so-called *modified long-wave approximation* (MLWA)^{17,19,22–34}. The MLWA^{17,19,22–34}, which can be viewed as a next-order approximation beyond the Rayleigh limit, is known to overcome a number of severe deficiencies of the Rayleigh limit (see eqn (2) below) and, at least for nonabsorbing hosts, be surprisingly precise^{17,19,27,31,33,34}.

The outline of our contribution is as follows. Section 2 first recalls in its Subsection 2.1 the expression for distance-independent apparent extinction cross section C_{ext} in the framework of the Lorenz–Mie theory¹³. In Subsection 2.2 our earlier developed MLWA^{33,34} is summarized. In Subsection 2.3, still within the framework of MLWA, an analytic first-order perturbation theory in a normalized extinction coefficient, $\bar{\kappa} = n_2''/n_2'$, representing the magnitude of the host dissipation, is developed. In Section 3, performance of the above approximations involving small plasmonic particles in different absorbing and active hosts is investigated. Discussion of some of the observed features is provided in Section 4. We then conclude with Section 5.

2 Theory

2.1 Apparent extinction cross section in the framework of the Lorenz–Mie theory

The specific expression for distance-independent apparent extinction cross section C_{ext} in the framework of the Lorenz–Mie theory is¹³ is given as an infinite sum over different multipole orders $\ell \geq 1$,

$$C_{\text{ext}} = -\frac{2\pi}{k'} \text{Re} \left\{ \sum_{\ell=1}^{\infty} \frac{1}{k} (2\ell+1)(T_{E\ell} + T_{M\ell}) \right\}. \quad (1)$$

In the optical convention, $T_{p\ell}$ correspond to the familiar Mie's expansion coefficients a_ℓ and b_ℓ (eqns (4.53) of ref. 2), i.e. $T_{E\ell} = -a_\ell$ for electric, or transverse magnetic (TM), polarization, and $T_{M\ell} = -b_\ell$ for magnetic, or transverse electric (TE), polarization. The physical, or operational, meaning of the distance-independent apparent C_{ext} is that it determines the reading of a polarization-sensitive well-collimated radiometer (WCR) at a sufficiently large distance r from the particle¹³,

$$\text{WCR signal} \propto \exp(-2k''r)(\Omega - C_{\text{ext}})I_{\text{inc}},$$

where Ω is the area of the objective lens of the WCR, and I_{inc} is the intensity of the incident homogeneous (uniform) plane wave at the center of the particle. Importantly, the distance-independent extinction cross-section *cannot* be introduced in the context of evaluating the energy budget of an arbitrarily shaped volume containing the scattering particle¹³.

2.2 The dipole MLWA

The MLWA is a rational approximation to the Mie coefficients in terms of a fraction of simple polynomials in size parameter x that in a concise way combines three different elementary terms, involving *size-independent* quasi-static Fröhlich term,

$$F_{p\ell} := v + \frac{\ell+1}{\ell},$$

the *dynamic depolarization* ($D_{p\ell} \sim x^2$) and the *radiative reaction* ($R_{p\ell} \sim x^{2\ell+1}$ for $p = E$ and $R_{p\ell} \sim x^{2\ell+3}$ for $p = M$) in the functional form^{17,19,22–34}

$$T_{p\ell} = \frac{iR_{p\ell}(x)}{F_{p\ell} + D_{p\ell}(x) - iR_{p\ell}(x)}. \quad (2)$$

Assuming nonmagnetic media, one has $v = \mu_1/\mu_2 = 1$ for magnetic (TE) polarization ($p = M$), and $v = \varepsilon := \varepsilon_1/\varepsilon_2$ for electric (TM) polarization ($p = E$), where the subscript 1 (2) identifies the relevant quantities of a sphere (host). The functional form of eqn (2) makes it transparent that the usual Rayleigh limit, which amounts to setting $D_{p\ell}(x) = R_{p\ell}(x) \equiv 0$ in the denominator for $\ell = 1$ and $p = E$, is recovered for $x, x_s \ll 1$. Here x is in general complex size parameter, $x = 2\pi a/\lambda$, with λ being the wavelength in the host medium, whereas $x_s = 2\pi n_2 a/n_1 \lambda = x/\sqrt{\varepsilon}$. The vanishing of the size-independent F in the denominator yields the usual quasi-static Fröhlich LSPR condition, which determines the quasi-static LSPR frequencies $\omega_{0\ell}$. In what follows, we shall focus

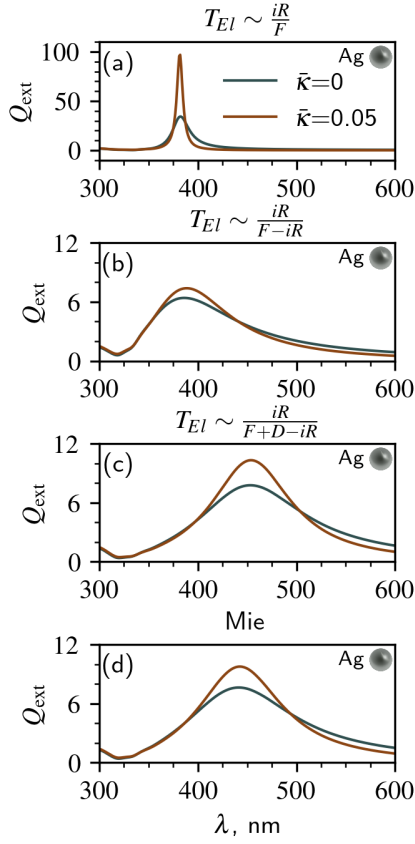


Fig. 2 Demonstration of different physical mechanisms described within MLWA on the extinction spectra of Ag sphere with $a = 40$ nm in the host with $n_2' = 1.33$. Here $\bar{\kappa} = 0$ for a transparent host and $\bar{\kappa} = 0.05$ in case of a dissipative host. The refractive indices of Ag were taken from ref. 35. (a) Quasi-static approximation; (b) radiative correction taking the effect of retardation with respect to the incident field; (c) the MLWA including additionally the dynamic depolarization term. Obviously all the correction terms of the dipole MLWA given by eqn (3) are necessary to achieve a fairly accurate approximation to the exact Mie theory shown in panel (d) for a comparison. All the above approximations, but the exact Mie theory, assume a constant field inside the sphere.

on the dipole MLWA which yields^{33,34}

$$T_{E1} \approx \frac{2i(\varepsilon - 1)x^3/3}{\varepsilon + 2 - 3(\varepsilon - 2)x^2/5 - 2i(\varepsilon - 1)x^3/3}, \quad (3)$$

where $\varepsilon = \varepsilon_1/\varepsilon_2$ is the relative dielectric function. An exceptional feature of the MLWA dipole contribution is that one can determine analytically an exact position of the complex pole of T_{E1} (the Mie coefficient $-a_1$), and hence the dipolar LSPR position, at

$$\varepsilon_{E1} = -2 \times \frac{1 + 3x^2/5 + ix^3/3}{1 - 3x^2/5 - 2ix^3/3}, \quad (4)$$

which corrects formula eqn (6) of ref. 19. The proof of that ε_{E1} yields complex zero of the denominator D of a_1 is relegated to Sec. S2 “Complex pole of the dipole contribution within the dipole MLWA” of ESI[†]. In the limit of small x , one can expand the denominator of ε_{E1} as $\sim 1 + 3x^2/5 + 2ix^3/3$, whereby eqn (4) reduces to the familiar classical Bohren and Huffman result (cf.

eqn (12.13) of ref. 2):

$$\varepsilon_{E1} \sim \varepsilon_{BH} \approx -2 - \frac{12x^2}{5} \quad (|x| \ll 1). \quad (5)$$

2.3 Perturbation theory in a normalized extinction coefficient within the MLWA

A useful parametrization of the relative dielectric function ε between the sphere and the host, suitable for studying the departure from nonabsorbing host, is (cf. eqn (9) of ref. 19):

$$\varepsilon = \frac{\varepsilon_1}{\varepsilon_2} = \frac{(n_1' + in_1'')^2}{(n_2' + in_2'')^2} = \frac{(n_1'/n_2' + in_1''/n_2'')^2}{(1 + in_2''/n_2')^2} = \frac{\varepsilon_t}{(1 + i\bar{\kappa})^2}, \quad (6)$$

where $\varepsilon_t = (n_1'/n_2' + in_1''/n_2'')^2 = \varepsilon_1/(n_2')^2$ is the relative (in general complex number if ε_1 is complex) dielectric function between the sphere and a *nonabsorbing* host with real refractive index n_2' , and $\bar{\kappa} = n_2''/n_2'$ is a normalized extinction coefficient representing the magnitude of the host dissipation. On substituting the Taylor expansion of the electric dipole term a_1 ,

$$a_1(\varepsilon) = a_1(\varepsilon_t) + \bar{\kappa} \left. \frac{da_1}{d\bar{\kappa}} \right|_{\varepsilon=\varepsilon_t} + \mathcal{O}(\bar{\kappa}^2),$$

in the expression eqn (1) of the apparent cross section, C_{ext} , it is in principle possible to provide in a systematic way the results for the extinction efficiency, $Q_{\text{ext}} = C_{\text{ext}}/\pi a^2$, in the first order of $\bar{\kappa}$ for both gain and absorbing media in the dipole approximation. The derivative $da_1/d\bar{\kappa}$ is determined by eqn (S21) of ESI[†] (Section S5: “The derivative $da_1/d\bar{\kappa}$ ”),

$$\frac{da_1}{d\bar{\kappa}} = -12n_2'x' \bar{\kappa} \text{Re} \left[\frac{2 - \varepsilon_t(\varepsilon_t - 1) + \frac{1}{5}(\varepsilon_t^2 - \varepsilon_t + 2)(x')^2}{n_2D^2(\varepsilon_t, x')} \right], \quad (7)$$

where $x' = x_0n_2'$, with $x_0 = 2\pi a/\lambda$ being the size parameter in vacuum host, and

$$D(\varepsilon_t, x') = \varepsilon_t + 2 - 3(\varepsilon_t - 2)(x')^2/5 - 2i(\varepsilon_t - 1)(x')^3/3 \quad (8)$$

is the denominator D in eqn (3) in the limit $\bar{\kappa} \rightarrow 0$. One finds eventually

$$\begin{aligned} Q_{\text{ext}} &= \frac{C_{\text{ext}}}{\pi a^2} \approx \frac{2}{x'} \text{Re} \left\{ \frac{3}{x} \left[a_1(\varepsilon_t) + \bar{\kappa} \left. \frac{da_1}{d\bar{\kappa}} \right|_{\varepsilon=\varepsilon_t} \right] \right\} \\ &= \frac{2}{x'} \text{Re} \left\{ \frac{3}{x} a_1(\varepsilon_t) \right\} - \\ &12n_2'x' \bar{\kappa} \text{Re} \left[\frac{2 - \varepsilon_t(\varepsilon_t - 1) + \frac{1}{5}(\varepsilon_t^2 - \varepsilon_t + 2)(x')^2}{n_2D^2(\varepsilon_t, x')} \right], \quad (9) \end{aligned}$$

which defines the first order expansion of Q_{ext} in the parameter $\bar{\kappa}$ within the perturbation theory (PT). The first term on the rhs is the dipole MLWA in a nonabsorbing host characterized by ε_t . The second term on the rhs is the perturbation correction. In what follows, we will refer to eqn (9) as the $\bar{\kappa}$ -PT approximation.

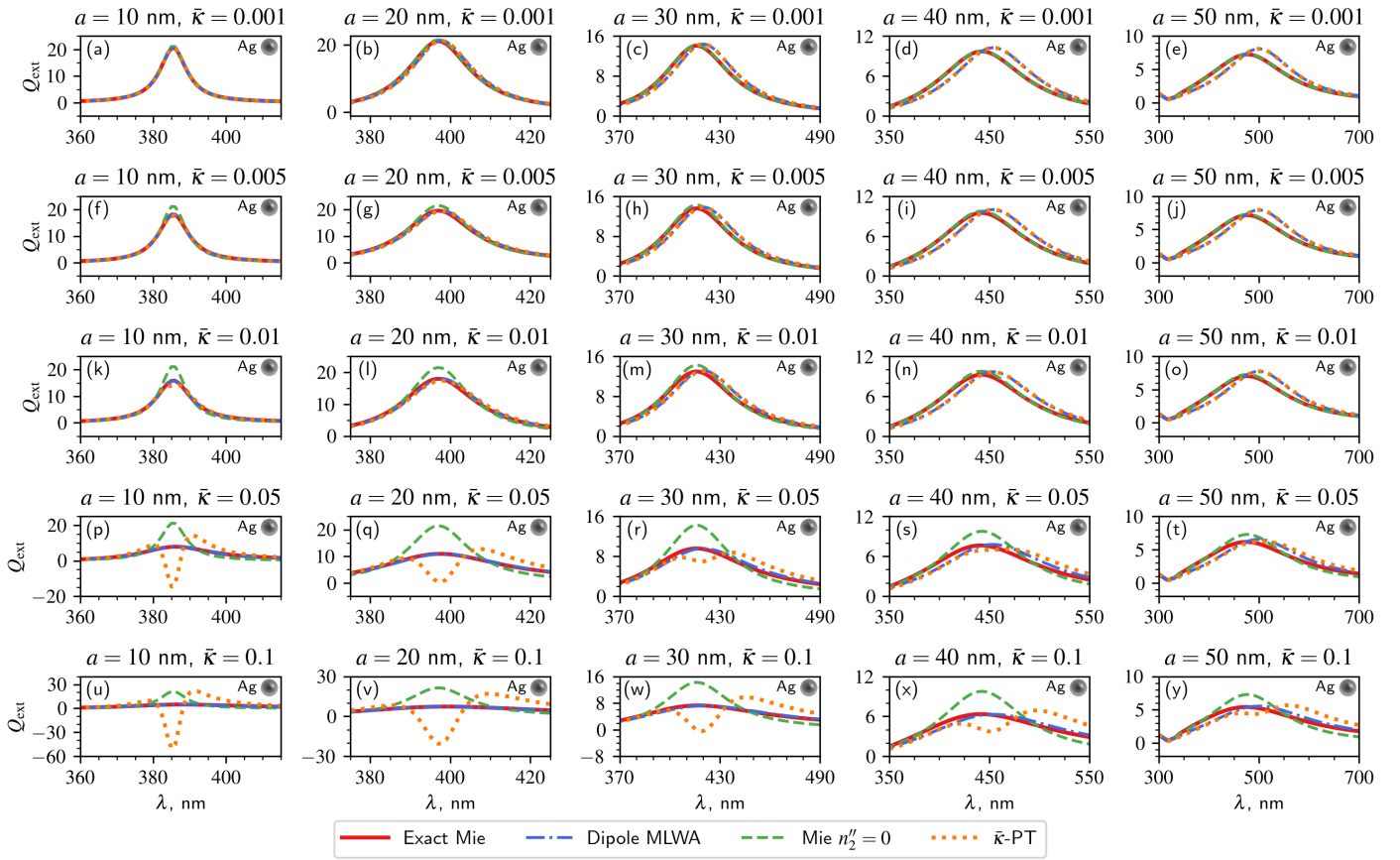


Fig. 3 Extinction spectra, Q_{ext} , for individual spherical Ag nanoparticles with radii $a = 10, 20, 30, 40, 50$ nm in water-like host ($n'_2 = 1.33$) with $\bar{\kappa} = 0.001, 0.005, 0.01, 0.05, 0.1$, as shown in the legend for each plot. Spectra were calculated by eqn (1) of the exact Mie theory (solid red line), the dipole MLWA by eqn (3) (blue dot-dashed line), the Mie theory in nonabsorbing host ($n''_2 = 0$; dashed green line), and the first order $\bar{\kappa}$ -PT of our eqn (9) (dotted orange line). Because the Mie theory in the nonabsorbing host is independent of $\bar{\kappa}$, its plots are identical at each given column. The refractive indices of Ag were taken from ref. 35.

3 Results

3.1 The dipole MLWA vs perturbation theory

Fig. 3 compares performance of various approximations relative to the exact Mie theory involving

- the dipole MLWA (with the sole term T_{E1} in eqn (1) given by eqn (3))
- the Mie theory approximation with nonabsorbing host (determined by eqn (1) with $n''_2 = 0$)
- the first-order $\bar{\kappa}$ -PT given by eqn (9)

in water-like host ($n'_2 = 1.33$) for different host absorption characterized by different values of $\bar{\kappa}$ on the example of Ag spheres with radii between 10 and 50 nm. Fig. 4 compares results for spheres made from most common plasmonic materials Al, Ag, Au, Mg with radius $a = 30$ nm in water-like host ($n'_2 = 1.33$) with $\bar{\kappa} = 0.01$ and -0.01 (similar results for glass-like host ($n'_2 = 1.5$) are presented in Fig. S2I of ESI[†]). As demonstrated in those figures, the dipole MLWA can be very precise. In the case of Ag and Au nanoparticles, the dipole MLWA essentially overlies with the exact Mie theory results for $a \lesssim 25$ nm. The agreement, slightly better in the case of Au than Ag, continues to be acceptable up to $a \sim 50$

nm (Fig. S1III of ESI[†]), and can be used, at least qualitatively, up to $a \sim 70$ nm (Fig. S1IV of ESI[†]). In the case of Al and Mg nanoparticles, a slight deviation from Mie theory results becomes visible by the naked eye already for $a \gtrsim 25$ nm (cf. Figs. S1I and S1II of ESI[†]). The agreement continues to be acceptable up to $a \sim 40$ nm and can be used at least qualitatively up to $a \sim 50$ nm (Fig. S1III of ESI[†]).

A first general observation is that with increasing sphere radius the performance of the dipole MLWA worsens. This is not surprising, as the MLWA is by definition a long wavelength approximation. The same applies to the $\bar{\kappa}$ -PT. The $\bar{\kappa}$ -PT overlies with the dipole MLWA for all $a \leq 50$ nm, provided that $\bar{\kappa} \leq 0.01$. The latter justifies a posteriori that our $\bar{\kappa}$ -PT is correct. Another interesting tendency revealed by Fig. 3 (Figs. S1I and S1II of ESI[†]) is that the maximal radius a for which the dipole MLWA remains accurate increases with increasing $\bar{\kappa}$.

Importantly, the results of $\bar{\kappa}$ -PT and the dipole MLWA overlies with the exact Mie theory results for $a \lesssim 25$ nm, which supports earlier observation on the range of validity of the MLWA in an absorbing host by Khlebtsov¹⁷. Whereas the dipole MLWA continues to overlie with the exact Mie theory results for $a \lesssim 25$ nm irrespective of $\bar{\kappa}$, the results of the $\bar{\kappa}$ -PT begin to deviate from

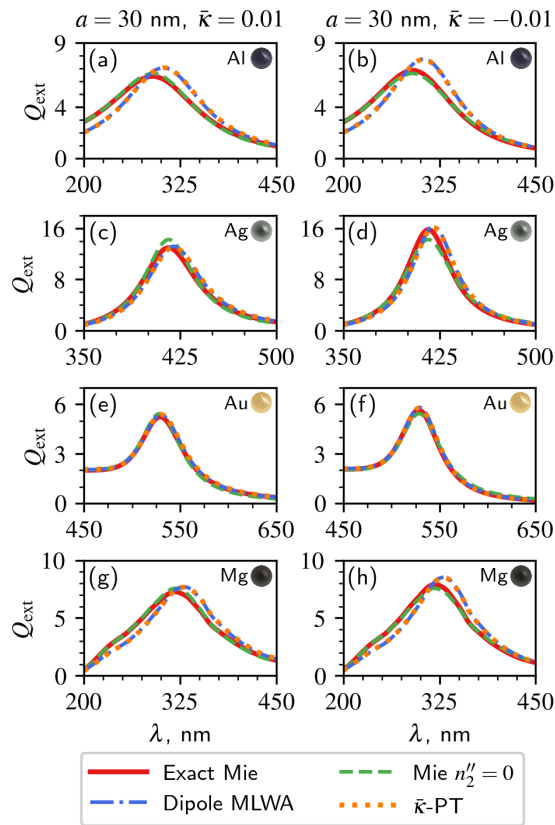


Fig. 4 Extinction spectra, Q_{ext} , for Al, Ag, Au and Mg spherical nanoparticles with $a = 30$ nm embedded in a host absorption medium with $n_2'' = 1.33$ (left column) and gain host medium (right column). The left (right) column is for $\bar{\kappa} = 0.01$ ($\bar{\kappa} = -0.01$). Q_{ext} are shown as calculated by eqn (1) of the Mie theory (solid red line), within dipole MLWA of eqn (3) (blue dot-dashed line), the Mie theory approximation with the nonabsorbing host (green dashed line), and by the $\bar{\kappa}$ -PT given by eqn (9) (dotted orange line). The refractive indices of Ag, Al, Au were taken from ref. 35 and those of Mg from ref. 36.

those of the dipole MLWA for $\bar{\kappa} \gtrsim 0.05$. This is to be expected, because the $\bar{\kappa}$ -PT is a first order perturbation theory of the dipole MLWA in $\bar{\kappa}$.

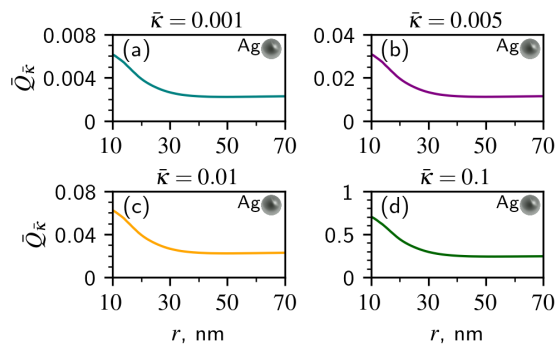


Fig. 5 Size dependence of $\bar{Q}_{\bar{\kappa}}$, the ratio of the PT correction to the leading term on the rhs of eqn (9), for Ag sphere at the (size-dependent) LSPR wavelength for different $\bar{\kappa}$: (a) 0.001, (b) 0.005, (c) 0.01 and (d) 0.1.

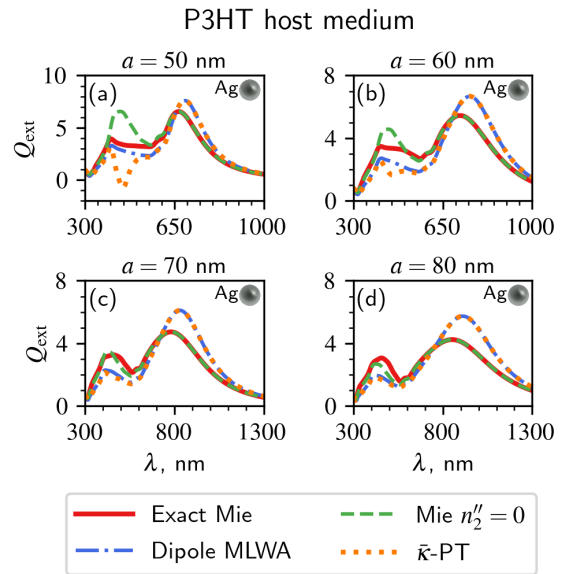


Fig. 6 Extinction spectra, Q_{ext} , for spherical Ag nanoparticles with (a) $a = 50$ nm, (b) $a = 60$ nm, (c) $a = 70$ nm, and (d) $a = 80$ nm embedded in Poly(3-hexylthiophene) (P3HT) host medium. Spectra are shown as calculated with the exact Mie theory (solid red line), the Mie theory for non-absorbing media ($n_2'' = 0$) (green dashed line), the dipole MLWA (blue dot-dashed line), and the $\bar{\kappa}$ -PT (dotted orange line).

Surprisingly, the smaller the particle, the greater the deviation of the $\bar{\kappa}$ -PT relative to the dipole MLWA for $\bar{\kappa} \gtrsim 0.05$ (see Fig. S1 and S2 of ESI[†]). The origin of this behaviour is that $D(\epsilon_r)$ is typically small in a proximity of a LSPR (cf. the generalized Fröhlich condition eqn (5)). Whereas the first term in eqn (9) is of the order $1/D(\epsilon_r)$, the term proportional to $\bar{\kappa}$ is of the order $1/D^2(\epsilon_r)$. However, when the size parameter x increases, $|D(\epsilon_r)|$ at a LSPR decreases (due to a larger separation from the complex zero), and, as illustrated in Fig. 5, $\bar{Q}_{\bar{\kappa}}$, defined as the ratio of the PT correction to the leading term on the rhs of eqn (9), gradually decreases, whereby the first-order $\bar{\kappa}$ -PT begins to approximate the MLWA. Note also how the ratio $\bar{Q}_{\bar{\kappa}}$ increases with $\bar{\kappa}$, which, as expected, explains why the $\bar{\kappa}$ -PT begins to deviate from the MLWA with increasing $\bar{\kappa}$.

3.2 Mie theory approximation with nonabsorbing host

Similar behaviour is observed for the Mie theory approximation with nonabsorbing host ($n_2'' = 0$) that begins to deviate from the exact Mie theory results, but somewhat earlier, beginning with $\bar{\kappa} = 0.01$. Again the smaller the particle, the greater the deviation. Nevertheless, the Mie theory approximation with nonabsorbing host becomes the best approximation with increasing particle radius (e.g. $a \gtrsim 40$ nm and $\bar{\kappa} \leq 0.01$). For example, the Mie theory in nonabsorbing host begins to overlap with the Mie theory in an absorbing host for $a \gtrsim 50$ nm and $\bar{\kappa} = 0.01$ (see Fig. S1 of ESI[†]). A threshold radius for which it happens increases with $\bar{\kappa}$.

Why the Mie theory approximation with nonabsorbing host becomes the best approximation for sufficiently large a can be explained by increasing relevance of higher-order multipole contributions with increasing particle size. This is understandable, be-

cause with increasing a higher order multipoles, which are obviously absent in any dipole approximation, become more and more relevant. This is demonstrated also in Fig. 6 showing the effect of increasing the radius of spherical Ag nanoparticles in Poly(3-hexylthiophene) (P3HT) host medium, which was used in a number of recent studies^{15,17,19,37}. Unlike inherent dipole approximations, the Mie theory approximation with nonabsorbing host captures reasonably well both the dipole and quadrupole peaks. Obviously, higher-order MLWA of ref. 34 could have captured the quadrupole peak, but this goes beyond the scope of present study.

3.3 Isolating the host dissipative effects on the extinction cross sections

The dissipative effects of the host on the extinction cross sections, Q_{ext} , can obviously be isolated by subtracting from the exact value $Q_{\text{ext}} = Q_{\text{ext};\varepsilon}$ the value of $Q_{\text{ext};\varepsilon_r}$ obtained by the Mie theory for the non-absorbing host characterised by $n_2'' = 0$ (i.e. $\varepsilon \rightarrow \varepsilon_r$). In what follows, we denote the difference by $\eta_{\text{eff}} := Q_{\text{ext};\varepsilon} - Q_{\text{ext};\varepsilon_r}$. Thus η_{eff} quantifies the contribution of the host absorption or gain in the resulting Q_{ext} . To our satisfaction, it turns out that, in a suitable parameter range, the analytic $\bar{\kappa}$ -PT can reliably capture the effect of the host absorption on the extinction efficiency of a plasmonic nanosphere as demonstrated in Fig. 7. Not surprisingly, the agreement can also be reached in the case of gain media, which opens door for analysis of promising applications involving active media, see Fig. 4 (Fig. S5 of ESI[†]) such as spasers^{38–40}. Therefore, within the range of its validity, the first order $\bar{\kappa}$ -PT allows one to both intuitively and analytically understand the mechanisms of host dissipation or gain on the extinction efficiency of a plasmonic nanosphere.

4 Discussion

Rather exhaustive MLWA analysis in the absorbing case has been recently provided by Khlebtsov¹⁷ by employing slightly different MLWA. The study of ref. 17 arrived at similar conclusions that MLWA is very precise for $a \lesssim 25$ nm. Our study complements ref. 17 with (i) a first order analytic perturbation theory around a nonabsorbing host in a normalized extinction coefficient $\bar{\kappa}$ ($\bar{\kappa}$ -PT) and (ii) an investigation of gain media. In addition, we have examined the behaviour of Al and Mg nanoparticles.

5 Conclusions

Our previously developed modified dipole long-wave approximation (MLWA) was shown to essentially overly with the exact Mie theory results for $a \lesssim 25$ nm ($a \lesssim 20$ nm) in the case of Ag and Au (Al and Mg) nanoparticles. The agreement for Au and Ag (Al and Mg) nanoparticles, slightly better in the case of Au than Ag, continues to be acceptable up to $a \sim 50$ nm ($a \sim 40$ nm), and can be used, at least qualitatively, up to $a \sim 70$ nm ($a \sim 50$ nm). We developed within the dipole MLWA a first order analytic perturbation theory (PT) around a nonabsorbing host in a normalized extinction coefficient $\bar{\kappa}$ and investigated its properties. It was shown that, in a suitable parameter range, the $\bar{\kappa}$ -PT can reliably capture the effect of host absorption or gain on the extinction efficiency of a plasmonic nanosphere. Considering growing interest

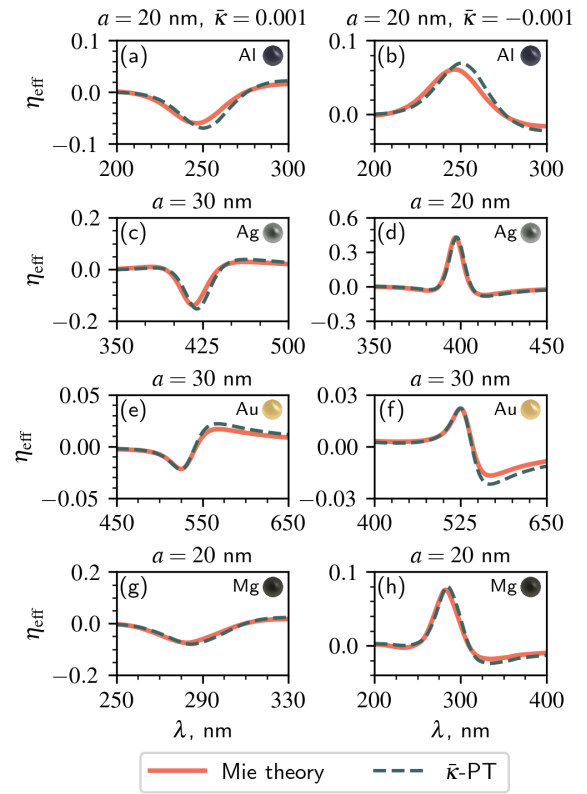


Fig. 7 The effect η_{eff} of the host absorption (left column) and the gain host medium (right column) on Q_{ext} in the Mie theory (solid red line) and the $\bar{\kappa}$ -PT (dashed dark green line) for Al, Ag, Au and Mg materials with different radii a embedded in the host medium with $n_2' = 1.33$ and $\bar{\kappa} = 0.001$ (left column) and $\bar{\kappa} = -0.001$ (right column).

in light-matter interactions, we expect that our results will help in designing optimal systems comprising plasmonic nanoparticles embedded in suitable dissipative or gain media for various applications.

Author Contributions

Conflicts of interest

There are no conflicts to declare.

Acknowledgements

Electronic Supplementary Information

The supplementary information includes Sec. S1 “Supplementary Figures”, where additional visual data are provided on apparent extinction efficiencies for further particle radii, host n_2' , and normalized extinction coefficient $\bar{\kappa}$. In Sec. S2 “Complex Pole of the Dipole Contribution within the Dipole MLWA”, the predictive power of the complex pole knowledge on the LSPR position is investigated. Sec. S3 “Proof of that ε_{E1} is the Complex Zero of the Denominator of a_1 ” presents mathematical proof of what is in its title. In Sec. S4 “The Imaginary Part of ε_{E1} is Negative” proves the stated statement for any real x . In Sec. S5 “The Derivative $da_1/d\bar{\kappa}$ ” explicit calculations leading to eqn (7) are presented. Sec. S6 “A Previous Attempt to Formulate a Perturbation The-

ory (PT) in Terms of $\bar{\kappa}$ ” analyses an earlier failed theoretical attempt. Sec. S7 “Apparent Extinction Cross Section” reviews the absorption and scattering cross-sections within the MLWA. Finally, Sec. S8 “Conventional Scattering Theory” reviews some related aspects of conventional scattering theory.

Notes and references

- 1 R. G. Newton, *Scattering Theory of Waves and Particles*, Springer Berlin Heidelberg, Berlin, Heidelberg, 1982.
- 2 C. F. Bohren and D. R. Huffman, *Absorption and Scattering of Light by Small Particles*, Wiley-VCH Verlag GmbH & Co. KGaA, 1998.
- 3 R. Fuchs and K. L. Kliewer, *J. Opt. Soc. Am.*, 1968, **58**, 319–330.
- 4 W. C. Mundy, J. A. Roux and A. M. Smith, *J. Opt. Soc. Am.*, 1974, **64**, 1593–1597.
- 5 P. Chýlek and R. G. Pinnick, *Appl. Opt.*, 1979, **18**, 1123–1124.
- 6 C. F. Bohren and D. P. Gilra, *J. Colloid Interface Sci.*, 1979, **72**, 215–221.
- 7 A. N. Lebedev, M. Gartz, U. Kreibig and O. Stenzel, *Eur. Phys. J. D.*, 1999, **6**, 365–373.
- 8 I. W. Sudiarta and P. Chylek, *J. Opt. Soc. Am. A*, 2001, **18**, 1275–1278.
- 9 P. Yang, B.-C. Gao, W. J. Wiscombe, M. I. Mishchenko, S. E. Platnick, H.-L. Huang, B. A. Baum, Y. X. Hu, D. M. Winker, S.-C. Tsay and S. K. Park, *Appl. Opt.*, 2002, **41**, 2740–2759.
- 10 Q. Fu and W. Sun, *J. Quant. Spectrosc. Radiat. Transf.*, 2006, **100**, 137–142.
- 11 M. I. Mishchenko, *Opt. Express*, 2007, **15**, 13188–13201.
- 12 M. I. Mishchenko, G. Videen and P. Yang, *Opt. Lett.*, 2017, **42**, 4873–4876.
- 13 M. I. Mishchenko and P. Yang, *J. Quant. Spectrosc. Radiat. Transf.*, 2018, **205**, 241–252.
- 14 M. I. Mishchenko and J. M. Dlugach, *Appl. Opt.*, 2019, **58**, 4871–4877.
- 15 R. L. Peck, A. G. Brolo and R. Gordon, *J. Opt. Soc. Am. B*, 2019, **36**, F117–F122.
- 16 M. I. Mishchenko, M. A. Yurkin and B. Cairns, *OSA Continuum*, 2019, **2**, 2362–2368.
- 17 N. G. Khlebtsov, *Phys. Chem. Chem. Phys.*, 2021, **23**, 23141–23157.
- 18 J. Dong, W. Zhang and L. Liu, *Opt. Express*, 2021, **29**, 7690–7705.
- 19 S. Zhang, J. Dong, W. Zhang, Minggang Luo and L. Liu, *Opt. Lett.*, 2022, **47**, 5577–5580.
- 20 M. I. Mishchenko and J. M. Dlugach, *OSA Continuum*, 2019, **2**, 3415–3421.
- 21 G. Videen and W. Sun, *Appl. Opt.*, 2003, **42**, 6724–6727.
- 22 M. Meier and A. Wokaun, *Opt. Lett.*, 1983, **8**, 581–583.
- 23 E. J. Zeman and G. C. Schatz, *Dynamics on Surfaces*, Dordrecht, 1984, pp. 413–424.
- 24 E. J. Zeman and G. C. Schatz, *J. Phys. Chem.*, 1987, **91**, 634–643.
- 25 K. L. Kelly, E. Coronado, L. L. Zhao and G. C. Schatz, *J. Phys. Chem. B*, 2003, **107**, 668–677.
- 26 H. Kuwata, H. Tamaru, K. Esumi and K. Miyano, *Appl. Phys. Lett.*, 2003, **83**, 4625–4627.
- 27 A. Moroz, *J. Opt. Soc. Am. B*, 2009, **26**, 517–527.
- 28 I. Zorić, M. Zäch, B. Kasemo and C. Langhammer, *ACS Nano*, 2011, **5**, 2535–2546.
- 29 E. Massa, S. A. Maier and V. Giannini, *New J. Phys.*, 2013, **15**, 063013.
- 30 E. C. Le Ru, W. R. C. Somerville and B. Auguie, *Phys. Rev. A*, 2013, **87**, 012504.
- 31 D. Schebarchov, B. Auguie and E. C. Le Ru, *Phys. Chem. Chem. Phys.*, 2013, **15**, 4233–4242.
- 32 M. Januar, B. Liu, J.-C. Cheng, K. Hatanaka, H. Misawa, H.-H. Hsiao and K.-C. Liu, *J. Phys. Chem. C*, 2020, **124**, 3250–3259.
- 33 I. L. Rasskazov, P. S. Carney and A. Moroz, *Opt. Lett.*, 2020, **45**, 4056–4059.
- 34 I. L. Rasskazov, V. I. Zakomirnyi, A. D. Utyushev, P. S. Carney and A. Moroz, *J. Phys. Chem. C*, 2021, **125**, 1963–1971.
- 35 K. M. McPeak, S. V. Jayanti, S. J. P. Kress, S. Meyer, S. Iotti, A. Rossinelli and D. J. Norris, *ACS Photonics*, 2015, **2**, 326–333.
- 36 K. J. Palm, J. B. Murray, T. C. Narayan and J. N. Munday, *ACS Photonics*, 2018, **5**, 4677–4686.
- 37 R. Peck, A. Khademi, J. Ren, S. Hughes, A. G. Brolo and R. Gordon, *Phys. Rev. Research*, 2021, **3**, 013014.
- 38 D. J. Bergman and M. I. Stockman, *Phys. Rev. Lett.*, 2003, **90**, 027402.
- 39 N. M. Lawandy, *Appl. Phys. Lett.*, 2004, **85**, 5040–5042.
- 40 A. Veltri, A. Chipouline and A. Aradian, *Sci. Rep.*, 2016, **6**, 33018.

Electronic Supplementary Information: Intuitive understanding of extinction of small particles in absorbing and active host media within the MLWA

Anton D. Utyushev^{1,*}, Vadim I. Zakomirnyi², Alexey A. Shcherbakov¹, Ilia L. Rasskazov³, and Alexander Moroz⁴

¹*School of Physics and Engineering, ITMO University, 197101, Saint-Petersburg, Russia*

²*Beckman Institute for Advanced Science and Technology, University of Illinois at Urbana-Champaign, Urbana, IL 61801, USA*

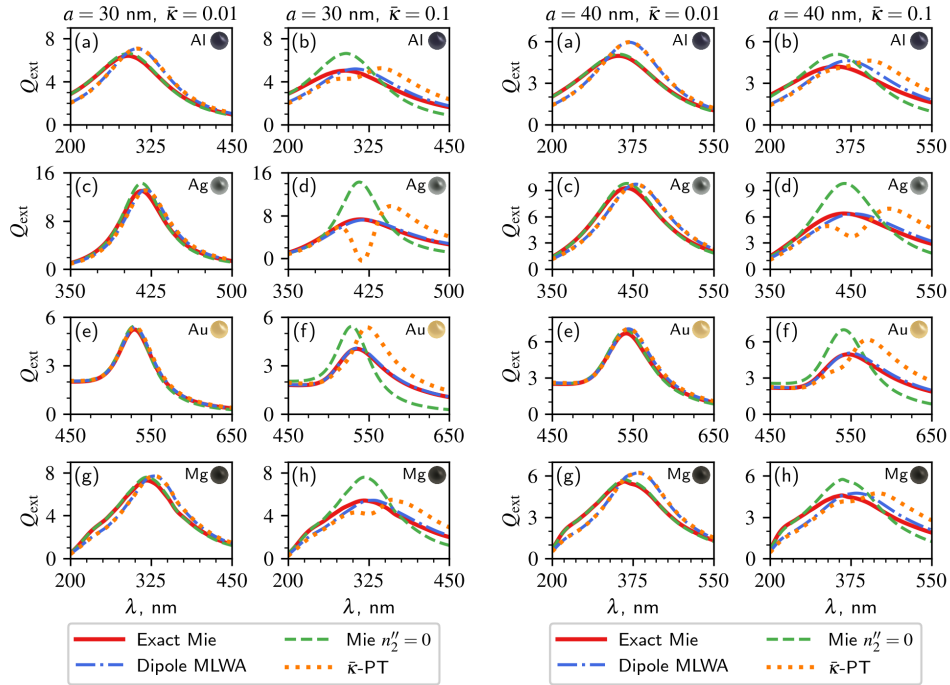
³*SunDensity Inc., Rochester, NY 14604, USA*

⁴*Wave-scattering.com*

*E-mail: ad.utyushev@gmail.com

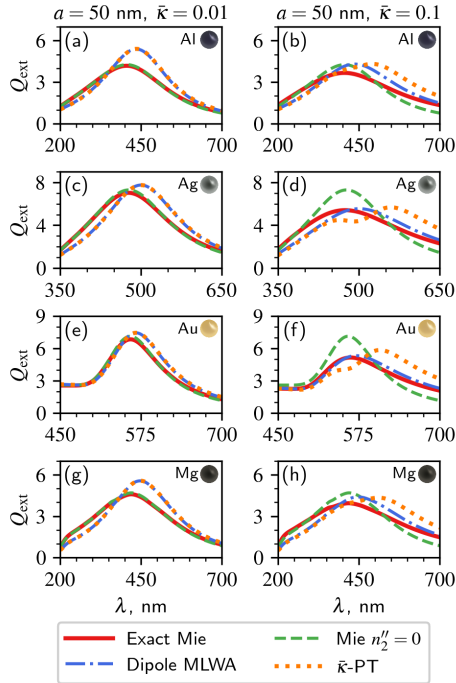
arXiv:2405.08903v1 [physics.optics] 14 May 2024

S1 Supplementary figures

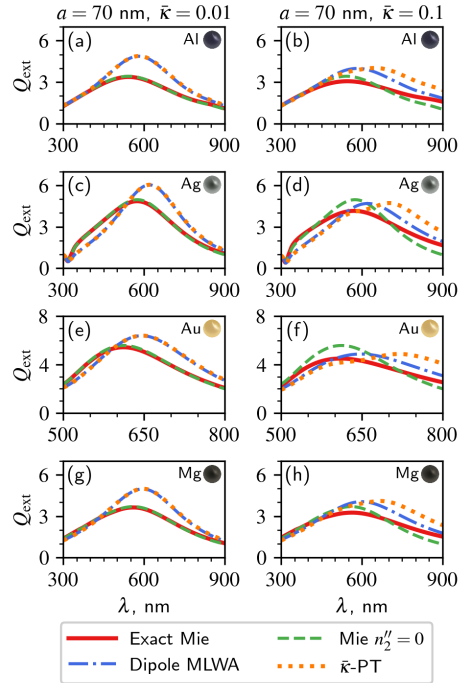


(I) $a = 30$ nm

(II) $a = 40$ nm

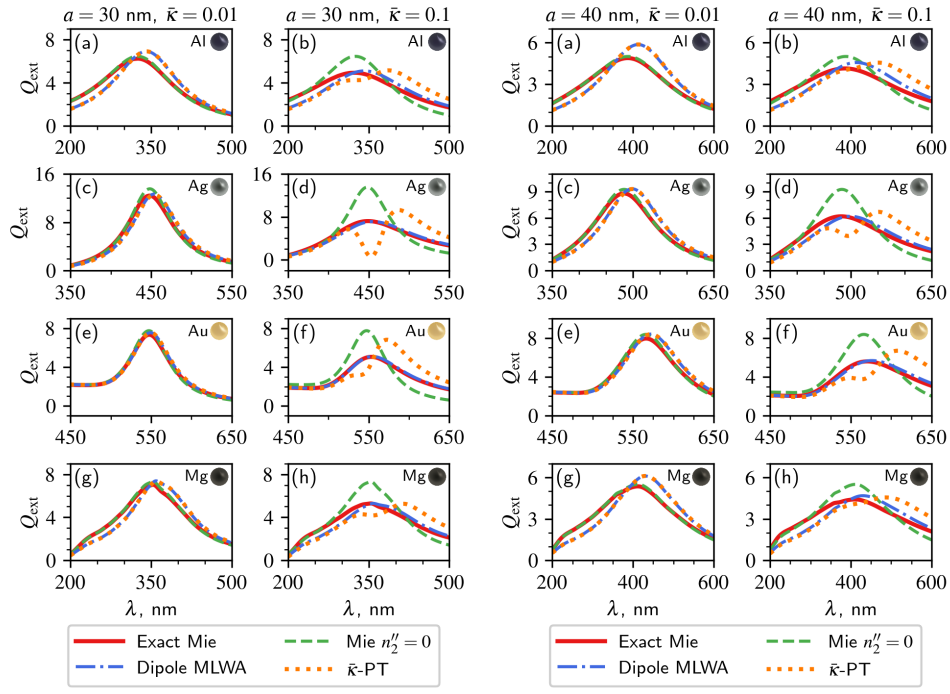


(III) $a = 50$ nm



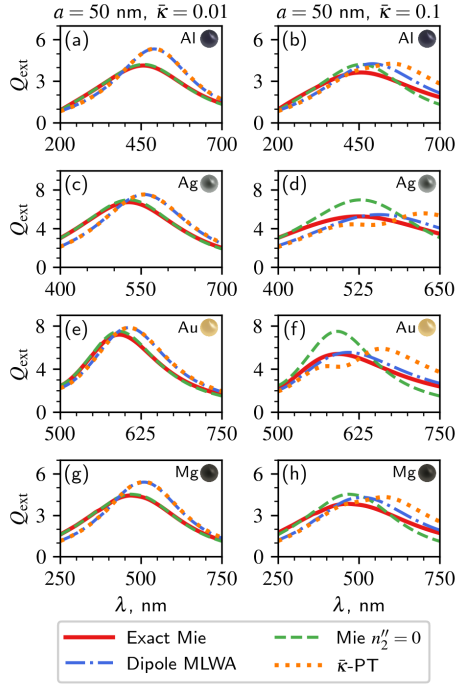
(IV) $a = 70$ nm

Figure S1 Extinction spectra, Q_{ext} , calculated with the exact Mie theory, the Mie theory for non-absorbing media ($n_2'' = 0$), the dipole MLWA, and the $\bar{\kappa}$ -PT for spherical nanoparticles of Al, Ag, Au and Mg with (I) $a = 40$ nm, (II) $a = 50$ nm, and (III) $a = 70$ nm. Absorbing host media have the real part of complex refractive index being that of water ($n_2' = 1.33$) and different values of imaginary part: $\bar{\kappa} = 0.01$ ($\bar{\kappa} = 0.1$) in the left (right) panel for any given a .

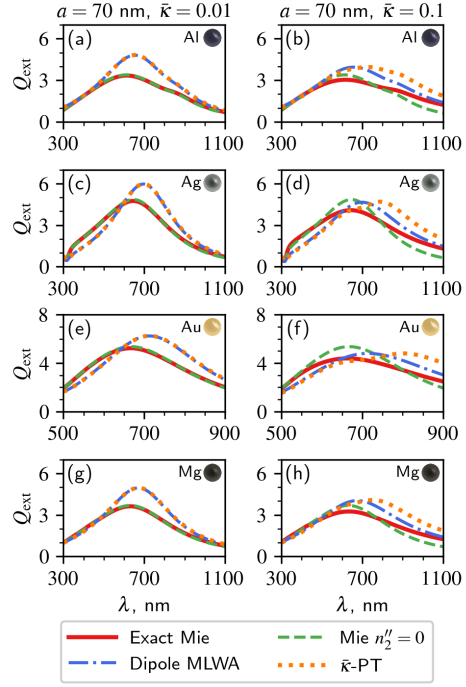


(I) $a = 30$ nm

(II) $a = 40$ nm



(III) $a = 50$ nm



(IV) $a = 70$ nm

Figure S2 Similarly to Fig. S1, but in $n_2'' = 1.5$ host media. The left (right) column for any given a is for $\bar{\kappa} = 0.01$ ($\bar{\kappa} = 0.1$).

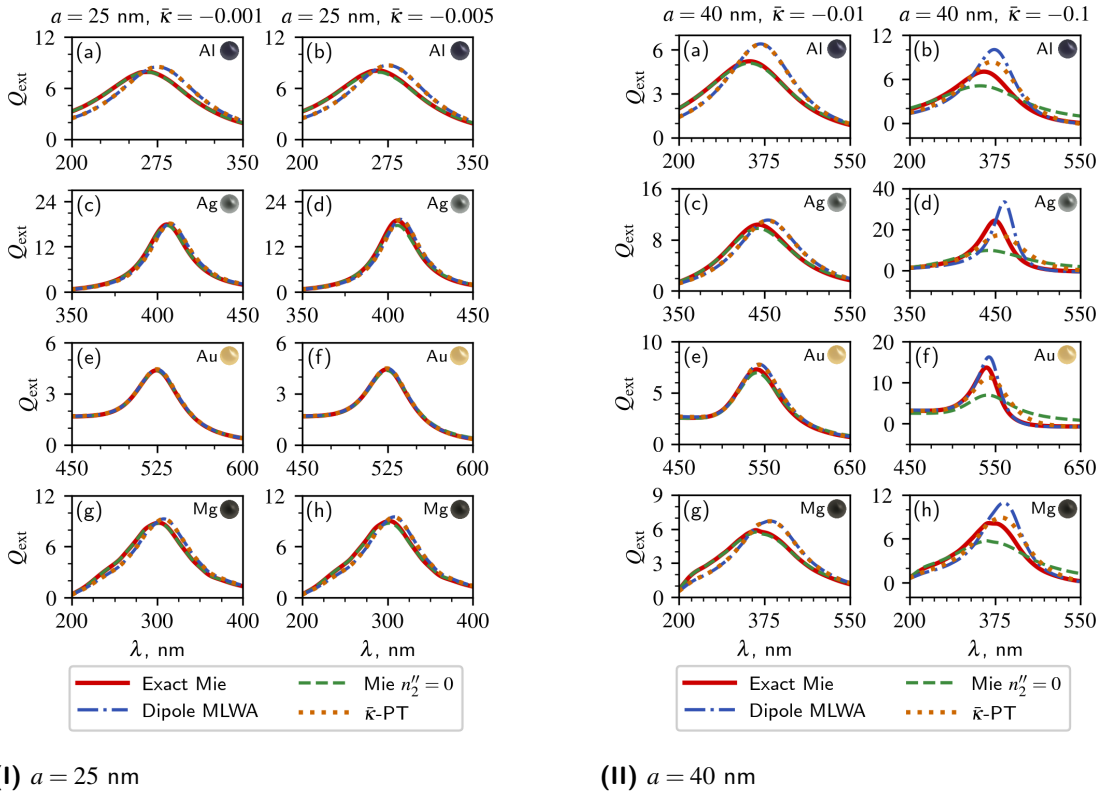


Figure S3 Extinction spectra, Q_{ext} , for spherical nanoparticles from Al, Ag, Au and Mg with (I) $a = 25$ nm, (II) $a = 40$ nm in the gain host media ($n_2' = 1.33$). The left (right) column is for any given $\bar{\kappa}$, calculated with the exact Mie theory (solid red line), the Mie theory approximation with non-absorbing host with $n_2'' = 0$ (dashed green line), the dipole MLWA (blue dot-dashed line), and by small $\bar{\kappa}$ perturbation theory (dotted orange line).

S2 Complex pole of the dipole contribution within the dipole MLWA

As stated in the main text, the exceptional feature of the MLWA dipole contribution is that one can determine analytically an exact position of the complex pole of the Mie coefficient a_1 at

$$\varepsilon_{E1} = -2 \times \frac{1 + 3x^2/5 + ix^3/3}{1 - 3x^2/5 - 2ix^3/3}, \quad (\text{S1})$$

which corrects eqn (6) of ref. 1. The proof of that ε_{E1} yields complex zero of the denominator of a_1 is relegated to Section S3. In the limit of small x one can expand the denominator of ε_{E1} as $\sim 1 + 3x^2/5 + 2ix^3/3$, whereby eqn (S1) reduces to the familiar classical result (cf. eqn (12.13) of ref. 2)

$$\varepsilon_{E1} \sim \varepsilon_{\text{BH}} \approx -2 - \frac{12x^2}{5} \quad (|x| \ll 1). \quad (\text{S2})$$

For a nonabsorbing host, the amended Fröhlich condition (eqn (S2)) has been used to explain the observed initial size-dependent red shift of the dipole localized surface plasmon resonance (LSPR)². Indeed ε_{BH} becomes more negative with increasing x , which for common Drude metals means that the LSPR is shifted to longer wavelengths. Surprisingly, the exact result (eqn (S1)) only marginally improves the amended Fröhlich condition (eqn (S2)). Actually the latter works better for $x \sim 1$.

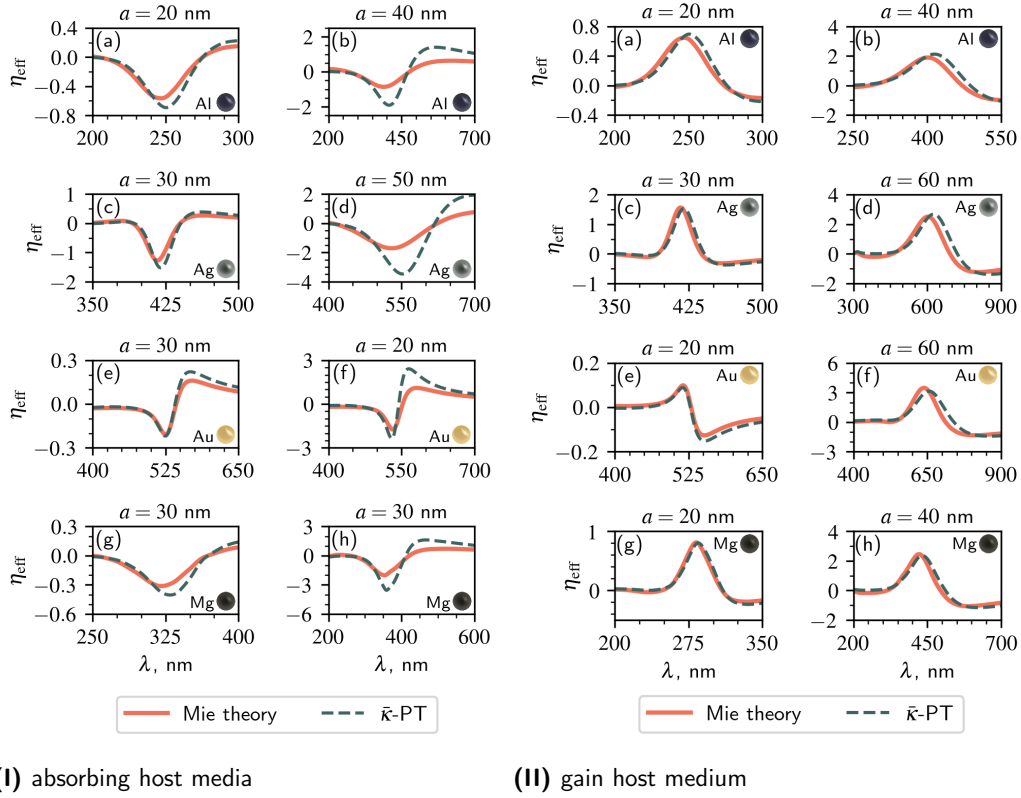


Figure S4 The effect η_{eff} of the host absorption on Q_{ext} in the Mie theory (full red line) and the $\bar{\kappa}$ -PT (dashed dark green line) for Al, Ag, Au and Mg materials with different radii a embedded in host medium with the left (right) column for any host medium $n_2' = 1.33$ ($n_2' = 1.5$) with (I) $\bar{\kappa} = 0.01$ ($\bar{\kappa} = 0.1$) and (II) $\bar{\kappa} = -0.01$ ($\bar{\kappa} = -0.1$). The figure supplements Fig. 7 of the main text, with the latter showing the results for $\bar{\kappa} = \pm 0.001$.

In order to use any of eqn (S1) or (S2) in practice, one has to notice that each of them does not define an isolated pole but rather a continuous line of poles, one for each given value of x . This is down to small x approximation, because the Mie coefficients in exact Mie theory have only discrete poles. Writing the relative dielectric function ε formally also with functional dependence on x , one can use eqn (S1) and (S2) for $|x| \lesssim 1$ to determine the absolute value of the difference $|\varepsilon(x) - \varepsilon_{E1}(x)|$. The minimum of $|\varepsilon(x) - \varepsilon_{E1}(x)|$ at some $x = x_r$ is expected to provide the dipole LSPR position. The resulting value of $\text{Im}(\varepsilon_{E1} - \varepsilon)$ at $x = x_r$ then determines the resonance linewidth (i.e. the FWHM). The latter presumes that at the absolute minimum $x = x_r$ of the difference of $|\varepsilon(x) - \varepsilon_{E1}(x)|$ it is justified to apply a pole approximation. More rigorously, on denoting by D the denominator of a_1 in eqn (3), one can approximate D around its zero as $D(x) \approx \varepsilon(x) - \varepsilon_{E1}(x_r)$. Consequently, near the complex zero of D one has

$$a_1 \approx -\frac{2i[\varepsilon(x) - 1]x^3/3}{\varepsilon(x) - \varepsilon_{E1}(x_r)}. \quad (\text{S3})$$

Obviously, the complex pole of a_1 is a point of maximum of a_1 (i.e. dipole LSPR). A distance from the real axis (i.e. $\text{Im}(\varepsilon_{E1} - \varepsilon)$) determines the resonance linewidth (i.e. the full width at half maximum (FWHM)). Had ε been a real quantity, then the resonance FWHM would be determined simply by $\text{Im} \varepsilon_{E1}$, i.e. the imaginary part of the complex pole as in the conventional scattering theory. Nonetheless it is difficult to obtain close analytic formulas for the FWHM.

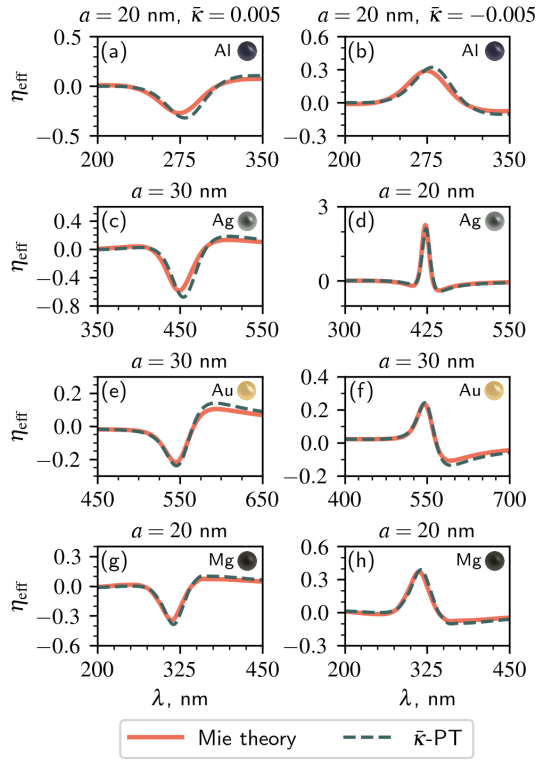


Figure S5 The effect η_{eff} of the host absorption (left column) and the gain host medium (right column) on Q_{ext} in the Mie theory (solid red line) and the $\bar{\kappa}$ -PT (dashed dark green line) for Al, Ag, Au and Mg materials with different radii a embedded in the host medium with $n'_2 = 1.5$ and $\bar{\kappa} = 0.005$ (left column) and $\bar{\kappa} = -0.005$ (right column). The figure supplements Fig. S4 and Fig 7 of the main text.

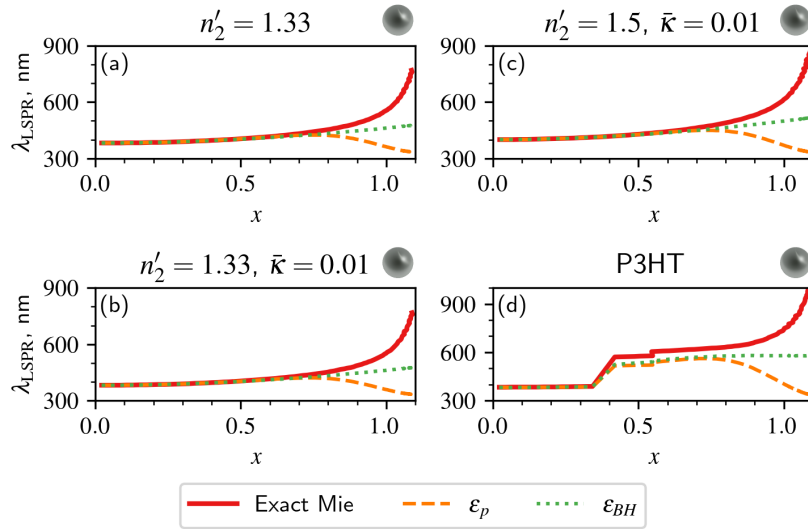


Figure S6 The LSPR positions predicted by the MLWA (eqn (S1) and eqn (S2)) relative to the exact Mie theory (eqn (1)) as functions of size parameter x .

S3 Proof of that ε_{E1} is the complex zero of the denominator of

a_1

Proof of that ε_{E1} given by eqn (S1) is an exact zero of the denominator of a_1 in the MLWA is as follows. On using eqn (S1), and on denoting $d = 1 - 3x^2/5 - 2ix^3/3$ the denominator of ε_{E1} in eqn (S1), one finds

$$\begin{aligned}
 \varepsilon_{E1} + 2 &= -\frac{2}{d} (1 + 3x^2/5 + ix^3/3 - 1 + 3x^2/5 + 2ix^3/3) \\
 &= -\frac{6}{d} (2x^2/5 + ix^3/3), \\
 3(\varepsilon_{E1} - 2) &= -\frac{6}{d} (1 + 3x^2/5 + ix^3/3 + 1 - 3x^2/5 - 2ix^3/3) \\
 &= -\frac{6}{d} (2 - ix^3/3), \\
 2(\varepsilon_{E1} - 1) &= -\frac{2}{d} (2 + 6x^2/5 + 2ix^3/3 + 1 - 3x^2/5 - 2ix^3/3) \\
 &= -\frac{6}{d} (1 + x^2/5). \tag{S4}
 \end{aligned}$$

On denoting D the denominator of a_1 in the MLWA (eqn (3)), then at $\varepsilon = \varepsilon_{E1}$

$$\begin{aligned}
 D &= -\frac{6}{d} [2x^2/5 + ix^3/3 - (x^2/5)(2 - ix^3/3) - i(x^3/3)(1 + x^2/5)] \\
 &= -\frac{6}{d} [i((x^2/5)x^3/3) - i((x^3/3)x^2/5)] \equiv 0. \tag{S5}
 \end{aligned}$$

S4 The imaginary part of ε_{E1} is negative

Here we show that the imaginary part of ε_{E1} given by eqn (S1) is negative for real x . One finds

$$\begin{aligned}
 \varepsilon_{E1} &= -\frac{2}{(1 - 3x^2/5)^2 + (2x^3/3)^2} \\
 &\quad \times (1 + 3x^2/5 + ix^3/3)(1 - 3x^2/5 + 2ix^3/3) \\
 &= -\frac{2}{(1 - 3x^2/5)^2 + (2x^3/3)^2} \\
 &\quad \times [1 - (3x^2/5)^2 - 2(x^3/3)^2 + i(x^3/3)(1 + x^2/5)]. \tag{S6}
 \end{aligned}$$

Hence

$$\text{Im } \varepsilon_{E1} = -\frac{(2/3)x^3(1 + x^2/5)}{(1 - 3x^2/5)^2 + (2x^3/3)^2} < 0. \tag{S7}$$

S5 The derivative $da_1/d\bar{\kappa}$

Taking into account κ -dependence of both ε (cf. eqn (6) of the main text) and of the size parameter $x = 2\pi an_2/\lambda$ through its explicit dependence on the complex refractive index $n_2 = n'_2(1 + i\kappa)$, the derivative $dT_{E1}/d\bar{\kappa}$ is calculated as

$$\frac{dT_{E1}}{d\bar{\kappa}} = \frac{\partial T_{E1}}{\partial \varepsilon} \frac{d\varepsilon}{d\bar{\kappa}} + \frac{\partial T_{E1}}{\partial x} \frac{dx}{d\bar{\kappa}}, \tag{S8}$$

where (cf. eqn (6))

$$\begin{aligned}
 \frac{d\varepsilon}{d\bar{\kappa}} &= -\frac{2i\varepsilon}{(1 + i\bar{\kappa})^3} \rightarrow -2i\varepsilon_i \quad (\bar{\kappa} \rightarrow 0), \\
 \frac{dx}{d\bar{\kappa}} &= in'_2x_0 = ix' \quad (\bar{\kappa} \rightarrow 0). \tag{S9}
 \end{aligned}$$

For the future convenience, we have introduced the size parameter in vacuum host, $x_0 = 2\pi a/\lambda$, leading to $x = n_2 x_0 = n'_2 x_0 (1 + i\bar{\kappa})$. On recalling eqn (3),

$$T_{E1} = \frac{2i(\varepsilon - 1)x^3/3}{\varepsilon + 2 - 3(\varepsilon - 2)x^2/5 - 2i(\varepsilon - 1)x^3/3}. \quad (\text{S10})$$

Now

$$\frac{\partial T_{E1}}{\partial x} = \frac{\frac{\partial u}{\partial x} D - u \frac{\partial D}{\partial x}}{D^2}, \quad (\text{S11})$$

where

$$u = \frac{2}{3}ix^3(\varepsilon - 1),$$

$$\frac{\partial u}{\partial x} = 2ix^2(\varepsilon - 1),$$

$$\frac{\partial u}{\partial \varepsilon} = \frac{2}{3}ix^3,$$

$$D = \varepsilon + 2 - \frac{3}{5}x^2(\varepsilon - 2) - \frac{2}{3}ix^3(\varepsilon - 1), \quad (\text{S12})$$

$$\frac{\partial D}{\partial x} = -\frac{6}{5}x(\varepsilon - 2) - 2ix^2(\varepsilon - 1),$$

$$\frac{\partial D}{\partial \varepsilon} = 1 - \frac{3}{5}x^2 - \frac{2}{3}ix^3,$$

$$\begin{aligned} u \frac{\partial D}{\partial x} &= \frac{2}{3}ix^3(\varepsilon - 1) \left[-\frac{6}{5}x(\varepsilon - 2) - 2ix^2(\varepsilon - 1) \right] \\ &= -\frac{4}{5}ix^4(\varepsilon - 1)(\varepsilon - 2) + \frac{4}{3}x^5(\varepsilon - 1)^2, \end{aligned}$$

$$\begin{aligned} \frac{\partial u}{\partial x} D &= 2ix^2(\varepsilon - 1) \left[\varepsilon + 2 - \frac{3}{5}x^2(\varepsilon - 2) - \frac{2}{3}ix^3(\varepsilon - 1) \right] \\ &= 2ix^2(\varepsilon - 1)(\varepsilon + 2) - \frac{6}{5}ix^4(\varepsilon - 1)(\varepsilon - 2) + \frac{4}{3}x^5(\varepsilon - 1)^2, \end{aligned}$$

$$\begin{aligned} \frac{\partial u}{\partial x} D - u \frac{\partial D}{\partial x} &= 2ix^2(\varepsilon - 1)(\varepsilon + 2) - \frac{6}{5}ix^4(\varepsilon - 1)(\varepsilon - 2) + \frac{4}{3}x^5(\varepsilon - 1)^2 \\ &\quad + \frac{4}{5}ix^4(\varepsilon - 1)(\varepsilon - 2) - \frac{4}{3}x^5(\varepsilon - 1)^2 \\ &= 2ix^2(\varepsilon + 2)(\varepsilon - 1) - \frac{2}{5}ix^4(\varepsilon - 1)(\varepsilon - 2), \end{aligned}$$

$$\frac{\partial T_{E1}}{\partial x} = 2ix^2(\varepsilon - 1) \frac{\varepsilon + 2 - \frac{1}{5}x^2(\varepsilon - 2)}{D^2}.$$

Taking the limit $\bar{\kappa} \rightarrow 0$

$$\lim_{\bar{\kappa} \rightarrow 0} \frac{\partial T_{E1}}{\partial x} \frac{dx}{d\bar{\kappa}} = -2(x')^3(\varepsilon_t - 1) \frac{\varepsilon_t + 2 - \frac{1}{5}(x')^2(\varepsilon_t - 2)}{D^2(\varepsilon_t, x')}, \quad (\text{S13})$$

where the functional dependence $D(\varepsilon_t, x')$ indicates that D in eqn (S12) is a function of ε_t and x' in the limit case.

Analogously,

$$\frac{dT_{E1}}{\partial \varepsilon} = \frac{\frac{\partial u}{\partial \varepsilon} D - u \frac{\partial D}{\partial \varepsilon}}{D^2}, \quad (\text{S14})$$

$$\begin{aligned} u \frac{\partial D}{\partial \varepsilon} &= \frac{2}{3} ix^3 (\varepsilon - 1) \left[1 - \frac{3}{5} x^2 - \frac{2}{3} ix^3 \right] \\ &= \frac{2}{3} ix^3 (\varepsilon - 1) - \frac{2}{5} ix^5 (\varepsilon - 1) + \frac{4}{9} x^6 (\varepsilon - 1), \end{aligned} \quad (\text{S15})$$

$$\begin{aligned} \frac{\partial u}{\partial \varepsilon} D &= \frac{2}{3} ix^3 \left[\varepsilon + 2 - \frac{3}{5} x^2 (\varepsilon - 2) - \frac{2}{3} ix^3 (\varepsilon - 1) \right] \\ &= \frac{2}{3} ix^3 (\varepsilon + 2) - \frac{2}{5} ix^5 (\varepsilon - 2) + \frac{4}{9} x^6 (\varepsilon - 1), \end{aligned} \quad (\text{S16})$$

$$\begin{aligned} \frac{\partial u}{\partial \varepsilon} D - u \frac{\partial D}{\partial \varepsilon} &= \frac{2}{3} ix^3 (\varepsilon + 2) - \frac{2}{5} ix^5 (\varepsilon - 2) + \frac{4}{9} x^6 (\varepsilon - 1) \\ &\quad - \frac{2}{3} ix^3 (\varepsilon - 1) + \frac{2}{5} ix^5 (\varepsilon - 1) - \frac{4}{9} x^6 (\varepsilon - 1) \\ &= 2ix^3 + \frac{2}{5} ix^5 = 2ix^3 \left(1 + \frac{1}{5} x^3 \right), \end{aligned} \quad (\text{S17})$$

$$\frac{\partial T_{E1}}{\partial \varepsilon} = 2ix^3 \frac{(1 + x^2/5)}{D^2}. \quad (\text{S18})$$

Taking the limit $\bar{\kappa} \rightarrow 0$

$$\lim_{\bar{\kappa} \rightarrow 0} \frac{\partial T_{E1}}{\partial \varepsilon} \frac{d\varepsilon}{d\bar{\kappa}} = 4\varepsilon_t (x')^3 \frac{1 + (x')^2/5}{D^2(\varepsilon_t, x')}. \quad (\text{S19})$$

On assembling the intermediary steps (S8), (S13), (S19) together,

$$\begin{aligned} \lim_{\bar{\kappa} \rightarrow 0} \frac{dT_{E1}}{d\bar{\kappa}} &= \lim_{\bar{\kappa} \rightarrow 0} \frac{\partial T_{E1}}{\partial x} \frac{dx}{d\bar{\kappa}} + \lim_{\bar{\kappa} \rightarrow 0} \frac{\partial T_{E1}}{\partial \varepsilon} \frac{d\varepsilon}{d\bar{\kappa}} \\ &= -2(x')^3 (\varepsilon_t - 1) \frac{\varepsilon_t + 2 - \frac{1}{5}(x')^2 (\varepsilon_t - 2)}{D^2(\varepsilon_t, x')} + 4\varepsilon_t (x')^3 \frac{1 + (x')^2/5}{D^2(\varepsilon_t, x')} \\ &= \frac{(x')^3}{D^2(\varepsilon_t, x')} \left\{ 4\varepsilon_t [1 + (x')^2/5] - 2(\varepsilon_t + 2)(\varepsilon_t - 1) + \frac{2}{5}(x')^2 (\varepsilon_t - 2)(\varepsilon_t - 1) \right\} \\ &= \frac{(x')^3}{D^2(\varepsilon_t, x')} \left\{ 4\varepsilon_t - 2(\varepsilon_t + 2)(\varepsilon_t - 1) + (2/5)(x')^2 [2\varepsilon_t + (\varepsilon_t - 2)(\varepsilon_t - 1)] \right\} \\ &= \frac{(x')^3}{D^2(\varepsilon_t, x')} \left\{ 4\varepsilon_t - 2(\varepsilon_t^2 + \varepsilon_t - 2) + (2/5)(x')^2 (2\varepsilon_t + \varepsilon_t^2 - 3\varepsilon_t + 2) \right\} \\ &= \frac{2(x')^3}{D^2(\varepsilon_t, x')} \left\{ 2 + \varepsilon_t - \varepsilon_t^2 + \frac{1}{5}(\varepsilon_t^2 - \varepsilon_t + 2)(x')^2 \right\}, \end{aligned} \quad (\text{S20})$$

and

$$\left. \frac{da_1}{d\bar{\kappa}} \right|_{\bar{\kappa} \rightarrow 0} = - \left. \frac{dT_{E1}}{d\bar{\kappa}} \right|_{\bar{\kappa} \rightarrow 0} = - \frac{2(x')^3}{D^2(\varepsilon_t, x')} \left\{ 2 + \varepsilon_t - \varepsilon_t^2 + \frac{1}{5}(\varepsilon_t^2 - \varepsilon_t + 2)(x')^2 \right\}. \quad (\text{S21})$$

Eventually,

$$\begin{aligned}
Q_{\text{ext}} &= \frac{C_{\text{ext}}}{\pi a^2} \approx \frac{2}{x'} \text{Re} \left\{ \frac{3}{x} \left[a_1(\varepsilon_t) + \bar{\kappa} \left. \frac{da_1}{d\bar{\kappa}} \right|_{\varepsilon=\varepsilon_t} \right] \right\} \\
&= \frac{2}{x'} \text{Re} \left\{ \frac{3}{x} a_1(\varepsilon_t) \right\} - 12n_2' x' \bar{\kappa} \text{Re} \left[\frac{1}{n_2 D^2(\varepsilon_t, x')} \left\{ 2 - \varepsilon_t(\varepsilon_t - 1) + \frac{1}{5}(\varepsilon_t^2 - \varepsilon_t + 2)(x')^2 \right\} \right],
\end{aligned} \tag{S22}$$

where we have made use of that $x' = x_0 n_2'$ is a real number and $x'/x = n_2'/n_2$, where $n_2 = n_2' + in_2''$ is the complex refractive index. Eqn (S22) defines the first order perturbation expansion (PT) of Q_{ext} in the parameter $\bar{\kappa}$ in the main text. We remind here that ε_t is in general a complex number and, like n_2 in the denominator, cannot be taken in front of the Re sign.

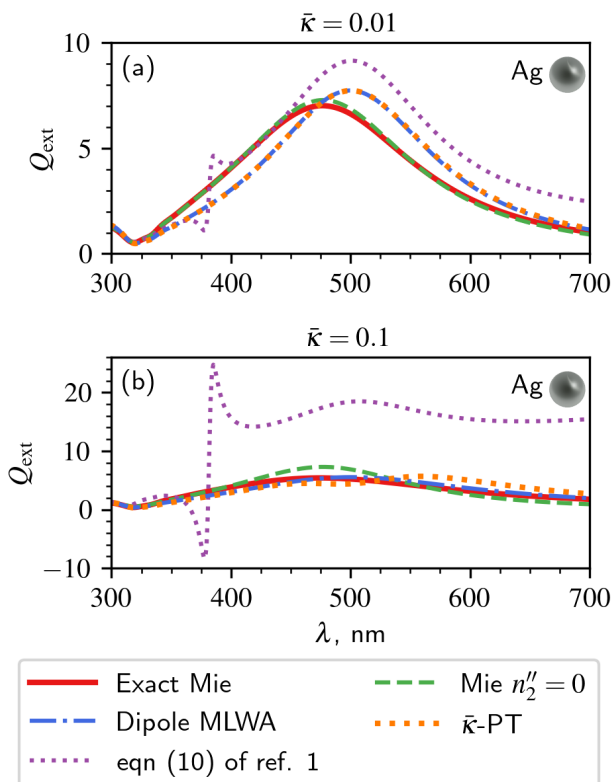


Figure S7 Extinction spectra, Q_{ext} , for spherical Ag particles with radius $a = 50$ nm embedded in host medium with (a) $n_2 = 1.33 + 0.0133i$ and (b) $n_2 = 1.33 + 0.133i$, calculated by eqn (1) of the Mie theory (solid red line), the Mie theory in nonabsorbing host with $n_2'' = 0$ (green dashed line), the dipole MLWA of eqn (3) (blue dot-dashed line), and the $\bar{\kappa}$ -PT of our eqn (9) (dotted orange line). Small $\bar{\kappa}$ -PT given by eqn (10) of ref. 1 is shown in velvet dotted line.

S6 A previous attempt to formulate a perturbation theory (PT) in terms of $\bar{\kappa}$

A first attempt to formulate a PT in terms of $\bar{\kappa}$ has been performed earlier in ref. 1. However we could neither reproduce their analytic results nor confirm that they are in any sense reliable. For the sake of comparison, Fig. S7 displays a comparison of the respective PT's against the exact Mie theory. The small $\bar{\kappa}$ approximation, given earlier by eqn (10) of ref. 1 and shown in the

velvet dotted line, performs worst and fails dramatically for $\bar{\kappa} = 0.1$. The cause of it is seen in a computational error.

S7 Apparent extinction cross section

In order to accommodate the changes for an *absorbing* host, we have to recast the extinction cross sections as

$$\begin{aligned}\sigma_{\text{ext};p\ell} &= -\frac{2\pi(2\ell+1)}{k'} \operatorname{Re} \left(\frac{1}{k} \frac{iR(x)}{F + D(x) - iR(x)} \right) \\ &= \frac{2\pi(2\ell+1)}{k'} \operatorname{Im} \left(\frac{1}{k} \frac{R(x)}{F + D(x) - iR(x)} \right).\end{aligned}\quad (\text{S23})$$

Within the dipole (i.e. $\ell = 1$) MLWA^{3,4} the above cross-sections take on the following form:

$$\sigma_{\text{sca};1} = \frac{4\pi}{15k^2} \frac{10x^6 |\tilde{\epsilon}_1 - 1|^2}{|\tilde{\epsilon}_1 + 2 - \frac{3}{5}(\tilde{\epsilon}_1 - 2)x^2 - i\frac{2}{3}(\tilde{\epsilon}_1 - 1)x^3|^2}, \quad (\text{S24})$$

$$\sigma_{\text{abs};1} = \frac{4\pi}{15k^2} \frac{9x^3 (x^2 + 5) \operatorname{Im}(\tilde{\epsilon}_1)}{|\tilde{\epsilon}_1 + 2 - \frac{3}{5}(\tilde{\epsilon}_1 - 2)x^2 - i\frac{2}{3}(\tilde{\epsilon}_1 - 1)x^3|^2}, \quad (\text{S25})$$

$$\sigma_{\text{ext};1} = \frac{4\pi}{15k^2} \frac{9x^3 (x^2 + 5) \operatorname{Im}(\tilde{\epsilon}_1) + 10x^6 |\tilde{\epsilon}_1 - 1|^2}{|\tilde{\epsilon}_1 + 2 - \frac{3}{5}(\tilde{\epsilon}_1 - 2)x^2 - i\frac{2}{3}(\tilde{\epsilon}_1 - 1)x^3|^2}, \quad (\text{S26})$$

where $\operatorname{Im}(\tilde{\epsilon}_1)$ denotes the imaginary part of $\tilde{\epsilon}_1$. The higher order multipole MLWA can be treated similarly⁴.

S8 Conventional scattering theory

In conventional scattering theory, any given angular momentum ℓ and polarization p ($p = E$ for electric (or TM) polarization, and $p = M$ for magnetic (or TE) polarization) channel contributes the following partial amount to the resulting scattering, absorption, and extinction cross sections (eqns (2.135-8) of ref. 5),

$$\sigma_{\text{sca};p\ell} = \frac{2\pi(2\ell+1)}{k^2} |T_{p\ell}|^2, \quad (\text{S27})$$

$$\sigma_{\text{abs};p\ell} = -\frac{2\pi(2\ell+1)}{k^2} [|T_{p\ell}|^2 + \operatorname{Re}(T_{p\ell})], \quad (\text{S28})$$

$$\sigma_{\text{ext};p\ell} = -\frac{2\pi(2\ell+1)}{k^2} \operatorname{Re}(T_{p\ell}), \quad (\text{S29})$$

where $k = 2\pi/\lambda$ is the wavenumber, with λ being the incident wavelength in the *host medium*.

The resulting full cross sections are determined as an infinite sum

$$\sigma_{\text{sca}} = \sum_{p,\ell} \sigma_{\text{sca};p\ell}, \quad \sigma_{\text{abs}} = \sum_{p,\ell} \sigma_{\text{abs};p\ell}, \quad \sigma_{\text{ext}} = \sum_{p,\ell} \sigma_{\text{ext};p\ell}. \quad (\text{S30})$$

It is easy to verify that in each particular channel one has $\sigma_{\text{ext};p\ell} = \sigma_{\text{sca};p\ell} + \sigma_{\text{abs};p\ell}$. For sufficiently small spherical particles of radius a , the cross sections eqn (S30) are often approximated by the very first electric dipole ($\ell = 1, p = E$) term in the familiar Rayleigh limit,

$$T_{E1} \rightarrow T_{E1;R} = \frac{2ix^3}{3} \frac{\epsilon - 1}{\epsilon + 2} \quad (x \ll 1), \quad (\text{S31})$$

where $x = 2\pi a/\lambda$, with λ being the wavelength in the host medium, is the familiar size parameter². This enables one an intuitive understanding of small nanoparticles².

Obviously, the above eqns (S27)-(S29) require a *nonabsorbing* host. The traditional scattering theory neglects the host dissipation and gain^{2,5}, because those cases imply either vanishing or infinite scattering wave at the spatial infinity. Once k is a complex number, eqns (S27)-(S29) cannot be straightforwardly extended for $k'' \neq 0$, because the expressions yield cross sections as *complex* quantities.

In order to arrive at the extinction cross section in an absorbing host, Bohren and Gilra⁶ concluded that it is necessary to move the $1/k^2$ prefactor on the rhs of eqn (S29) under the Re sign (see eqn (11) in ref. 6). Another their peculiar observation was that $\sigma_{\text{ext}} \neq \sigma_{\text{sca}} + \sigma_{\text{abs}}$ ⁶. Nearly two decades later, Bohren and Gilra result⁶ was in 2018 corrected by eqn (45) of Mishchenko and Yang⁷ in that only the $1/k$ -prefactor on the rhs of eqn (S29) goes under the Re sign, whereas the second $1/k$ -prefactor remains before the real sign, but not as such, because it is, in general, a complex quantity, but as $1/k'$, where k' stands for the *real* part of k .

References

- [1] S. Zhang, J. Dong, W. Zhang, Minggang Luo and L. Liu, *Opt. Lett.*, 2022, **47**, 5577–5580.
- [2] C. F. Bohren and D. R. Huffman, *Absorption and Scattering of Light by Small Particles*, Wiley-VCH Verlag GmbH & Co. KGaA, 1998.
- [3] I. L. Rasskazov, P. S. Carney and A. Moroz, *Opt. Lett.*, 2020, **45**, 4056–4059.
- [4] I. L. Rasskazov, V. I. Zakomirnyi, A. D. Utyushev, P. S. Carney and A. Moroz, *J. Phys. Chem. C*, 2021, **125**, 1963–1971.
- [5] R. G. Newton, *Scattering Theory of Waves and Particles*, Springer Berlin Heidelberg, Berlin, Heidelberg, 1982.
- [6] C. F. Bohren and D. P. Gilra, *J. Colloid Interface Sci.*, 1979, **72**, 215–221.
- [7] M. I. Mishchenko and P. Yang, *J. Quant. Spectrosc. Radiat. Transf.*, 2018, **205**, 241–252.